Anthropogenic impacts on mud and organic carbon cycling

Check for updates

Thomas S. Bianchi [1] ✉, Lawrence M. Mayer [2], Joao H. F. Amaral[1,3], Sandra Arndt [4,5], Valier Galy [6], David B. Kemp [7], Steven A. Kuehl [8], Nicholas J. Murray [9] & Pierre Regnier[4]

Fine-grained muds produced largely from rock weathering at the Earth's surface have great influence on global carbon cycling. Mud binds and protects organic carbon (OC) from remineralization, and its organic loading controls the amounts, timescales and pathways of OC sequestration in sediments and soils. Human activities have resulted in marked changes (both increases and decreases) in mud accumulation and associated OC (mud–OC) loadings in different environments via altering organic matter inputs and reactivity. Such impacts on mud and mud–OC can be directly caused by activities such as damming and levee building, or indirectly result from human-induced climate change. Here we present a synthesis of impacts of human activities on the production, transfer and storage of mud–OC. In general, we find that anthropogenic climate warming has increased net fluxes of mud–OC in most of the systems discussed here (for example, mountain glaciers, land erosion, dam burial, river export, permafrost thaw, ice-sheet erosion and burial in margins), with uncertainties for tidal flats and floodplains, and probably net losses for coastal wetlands. Whether the anthropogenic mobilization of mud–OC results in more or less sequestration of OC is not known with the current data, as it is dependent on timescales that involve complex transient effects.

The importance of fine-grained mud in shaping Earth's climate history has stimulated broad interest in the geosciences[1,2], with focus on the associations between mud and organic carbon (mud–OC; Box 1) beginning in the mid-nineteenth century. Mud is a key medium that integrates the carbon cycle as initiated by rock weathering and soil erosion, followed by transport, transformation and sequestration/burial of mud–OC across diverse landscapes[3–5]. Mud has been linked with microbial evolution[6], relating it to past and future changes in weathering, biogeochemical cycles and climate[6]. Mudrocks represent about 60% of all sedimentary rocks in Earth's crust, and are the primary archive from which geologists reconstruct Earth's biotic and climatic history[7]. Mud's influence on Earth's carbon cycling and climate has accentuated since the Palaeozoic era (Supplementary Information).

Anthropogenic disturbances to mud and mud–OC cycling have probably occurred from the mid-to-late Holocene epoch[8], with the most rapid and profound effects occurring during the Great Acceleration, or Anthropocene (for example, ref. 9). Human activities alter the production, source-to-sink transport and fate of mud–OC via

[1]Department of Geological Sciences, University of Florida, Gainesville, FL, USA. [2]School of Marine Sciences, University of Maine, Walpole, ME, USA. [3]Earth System Science Program, Faculty of Natural Sciences, Universidad del Rosario, Bogota, Colombia. [4]BGeoSys, Department of Geosciences, Environment and Society, Université Libre de Bruxelles, Brussels, Belgium. [5]iC3, Center for Ice, Climate, Carbon and Cryosphere, UiT the Arctic University of Norway, Tromsø, Norway. [6]Department of Marine Chemistry and Geochemistry, Woods Hole Oceanographic Institution, Woods Hole, MA, USA. [7]State Key Laboratory of Biogeology and Environmental Geology and Hubei Key Laboratory of Critical Zone Evolution, School of Earth Sciences, China University of Geosciences, Wuhan, China. [8]Virginia Institute of Marine Science, William & Mary, Gloucester Point, VA, USA. [9]College of Science and Engineering, James Cook University, Townsville, Queensland, Australia. ✉e-mail: tbianchi@ufl.edu

BOX 1

Definitions of mud and mud–OC

'Mud' is a generic term used differently across scientific and technological disciplines. Here, we consider mud as the finer (<63 μm) components of soils and suspended and deposited sediments. Mud often associates with coarser-grained materials (for example, sand) to varying degrees, and 'muds' and 'mudstones' are sediments/rocks consisting largely of this finer component. Mud dominates incorporation of other biogeochemically important substances, such as OC, in sediments. We define mud–OC as OC physically associated with mud (for example, ref. 3). Mineral-associated OC (MAOC) and particulate OC (POC) are each contained in mud–OC, but also exist in coarser deposits or in suspension. The majority of OC in soil occurs as MAOC, and is generally proportional to mud content[111]. Most sedimentary OC concentrations are similarly related to grain size[112], and mudrocks dominate the sedimentary record[113]; therefore, mud–OC must also dominate global stocks of sedimentary OC. Petrogenic OC from eroded rocks largely represents fossilized mud–OC associated with clay minerals. Mud–OC occurs in many environments, and can comprise terrestrial, marine and petrogenic sources.

Mud concentrates and stabilizes OC across rocks, soils and sediments. Much mud–OC associates with clay and silt-sized minerals[114] or various metals, for example, iron and calcium, that derive from chemical and physical weathering. Cohesive aggregates develop via physical, chemical and biological mechanisms in soil, riverine and marine environments[107],

with densities between organic matter (OM) and minerals[115]. Aggregation of OM with fine-grained minerals is enhanced by the latter's high specific surface area (SSA) and particle abundance, and affects subsequent transport, settling and compaction. Aggregation can stabilize mud and appears to protect mud–OC against biological degradation[115,116], prolonging OC concentrations and compositions into the rock record[102,105].

The composition, chemical stability and small size of mud minerals enhance adsorption and occlusion[107]. Many bonding types drive adsorption, depending on factors such as local solutes and oxidation state[107], which can change OC reactivity. OC protection also results from its occlusion into compartments that affect access by biota, enzymes and oxidants[107–109] at length scales ranging from adsorption into nanometre- to micrometre-sized-pores, to occlusion into millimetre-scale anoxic microsites, to burial in centimetre- to decimetre-scale, muddy sediment of low permeability. Interactions between adsorption and occlusion make this protection complex[107]. Ratios of OC concentrations to SSA or fine-grained mineral content in bulk soils or sediments allow normalization of OC concentration to mud's protective capability, helping to assess how OC loading in mud changes during source-to-sink transport. Such ratios—for example, OC:SSA often in the range 0.4–1.0 mgC m^{-2}—respond to factors such as OC supply and oxygen availability[117]. Mud's ability to sequester OC will thus depend strongly on local conditions in the reactors between source and sink.
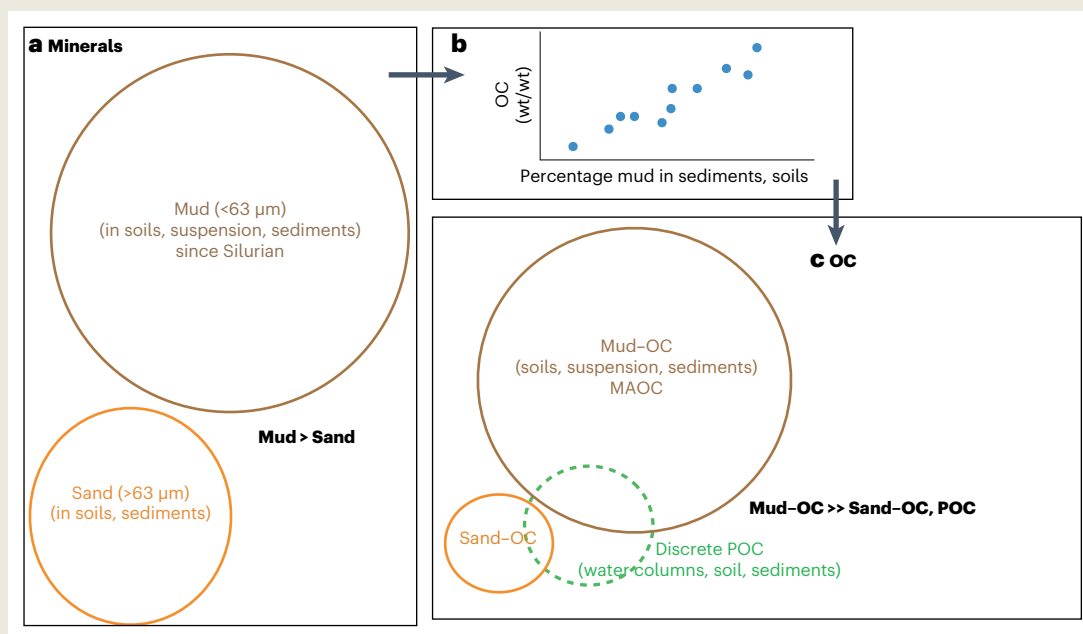
Mud control of mud–OC. a, There is more mineral mass as mud than sand in the post-Silurian geological record[112]. **b**, OC concentration increases with mud-sized mineral fraction of soils, sediments and rocks[3]. **c**, Mud–OC should therefore more strongly dominate global stocks of OC in suspension, soils, sediments and rock.

changes in land use (for example, deforestation, agriculture, mining, road building), water management (for example, damming, levees, groundwater withdrawal), perturbations of the coastal and deep ocean (dredging, trawling, offshore wind farms, aquaculture, mining), atmospheric CO_2 and climate (for example, droughts, floods, sea-level rise,

glacier retreat, permafrost thaw, terrestrial biosphere productivity). Because the fate of mud–OC can have substantial impacts on greenhouse gas fluxes and carbon sequestration/burial in the biosphere, important questions remain on how these anthropogenic changes will affect the carbon cycle and climate in the twenty-first century[10].
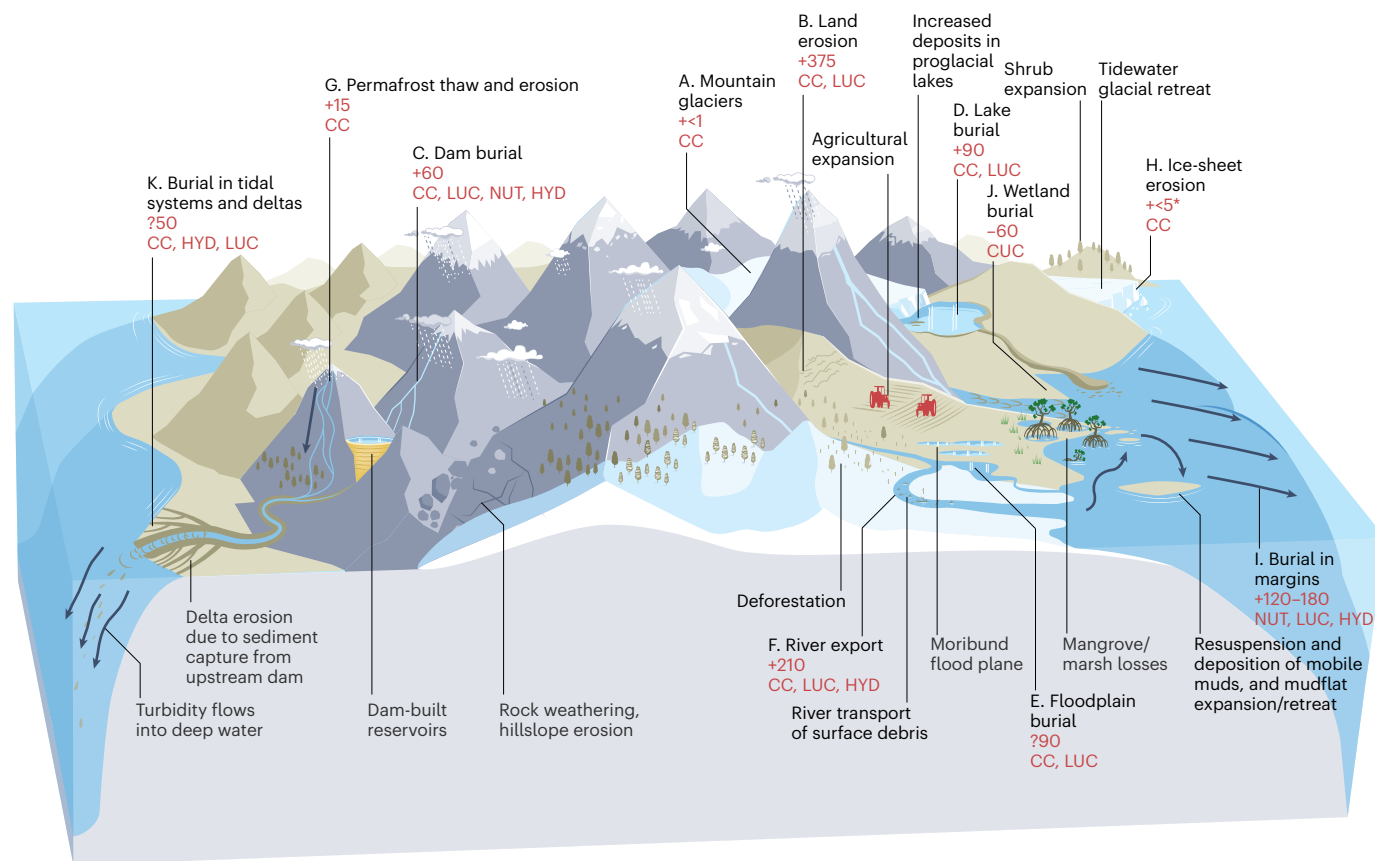
Fig. 1 | Major pathways of mud movement, POC fluxes and human-induced changes. The primary landscape processes controlling fluxes of mud and mud–OC (black text) influence mud–OC flux (red numbers) and their recent changes (+/−/?) via anthropogenic impacts (red abbreviations) along source-to-sink gradients. See Table 1 for references and further information associated with these fluxes. All fluxes are in TgC yr^{-1} rounded to ±5 TgC yr^{-1}. Note that the budget is not closed because it is partly constructed from independent estimates, the contribution of aquatic system metabolism to burial remains largely unknown, and the timescales of erosion, transport and burial are not uniformized. For instance, mud–OC burial on the continental shelves is timescale-dependent as shown quantitatively in refs. 100,101. The red text indicates notations present in Table 1. Processes/fluxes without numbers lack valid quantitative evidence.

Humans have altered the transit and hence distribution of mud between its weathering sources and its depositional sinks, dramatically changing its residence time along source-to-sink gradients[11–18]. Moreover, changing environmental conditions strongly influence the inputs, processing, remineralization and sequestration of mud–OC[19].

Here we review the state of knowledge about mobilization and storage of mud and its associated OC through dominant source-to-sink pathways (Fig. 1). We focus on Holocene–Anthropocene effects by human activities, which are altering production, transport and environmental conditions for mud–OC and therefore its exchange with pools such as the atmosphere. We emphasize mud–OC in permafrost, whose thawing mud enhances fluxes from land to sea in the Arctic (for example, ref. 4). Our main objectives are to: (1) assess how the dominant drivers of mud–OC production have changed over the Holocene–Anthropocene; (2) provide an overview of the large spatial and temporal changes in where mud–OC is remineralized and buried along the land-to-sea pathway, with potential consequences for carbon cycling and climate; and (3) explore how understanding of the fate of mud–OC can help predict consequences such as the recently accelerated release of ancient petrogenic and permafrost-derived OC to the biosphere.

The modern mud–OC cycle on land

Production of mud–OC in terrestrial ecosystems

Mud production requires weathering reactions, which change both particulate and dissolved materials (for example, feldspar to clay minerals and consequent increase in dissolved silica and various ions).

Mass budgets of mud are dominated by transfers among pre-existing mud deposits[11] (for example, soils and sediments) in different parts of the landscape—not new production of mud-sized minerals. Monitoring of dissolved ions to assess global weathering does not indicate Anthropocene increase in mud-producing reactions[11].

Despite little change in total available mud, erosion of mud–OC from ice-free landscapes in temperate regions has been substantially affected by land-use change over the Holocene–Anthropocene. Human agriculture has substantially increased global soil denudation since the late Holocene; an estimated ~36 Pg yr^{-1} of soil was eroded in 2012[12]. Currently, an estimated 37% of all ice-free land is directly used for agriculture and human settlements[13,14]. Impacts are most pronounced in the Northern Hemisphere, which hosts more land, human population and gross domestic product[12,14]. Soil loss and mud–OC mobilization due to anthropogenic land-use changes began >4,000 years ago[8,16]. In North America, the impact of European colonization on the landscape (via agriculture and river modifications) is readily observed, with rates of surficial sediment movement (and hence mud–OC mobilization) over the past century about ten times higher than pre-colonial rates[15]. Rates of deforestation and agricultural land expansion are now slowing or even reversing in the Northern Hemisphere, and accelerating in the Southern Hemisphere[17]. In Europe, climate change rather than land-use change is predicted to be the main driver of modest increases in soil erosivity in the coming decades[18]. Global land-surface models integrating vegetation dynamics suggest that enhanced plant growth driven by increased atmospheric CO_2 could partly mitigate the erosive effects of climate change via soil stabilization[20]. In contrast, substantial

Table 1 | The POC cycle in the Anthropocene, probably dominated throughout by mud–OC

Fig. 1 code	Landscape feature/process	Flux estimate (TgC yr⁻¹)	Flux with perturbation (+/−/?)	From	To	Perturbations	Reference
A	Mountain glaciers	<1	+	Land	Inland waters	CC	93
B	Land erosion	375	+	Land	Inland waters	CC, LUC	94
C	Dam burial	60	+	Land	Inland waters	CC, LUC, NUT, HYD	27,95
D	Lake burial	90	+	Land	Inland waters	CC, LUC	95
E	Floodplain burial	190	?	Land	Inland waters	CC, LUC, HYD	5,31
F	River export	210	+	Inland waters	Nearshore	CC, LUC, HYD	5,96
G	Permafrost thaw	14	+	Land	Nearshore	CC	54,58
H	Ice-sheet erosion	<5	+	Land	Margins	CC	97
I	Burial in margins	120–180	+	Land/nearshore	Margins	HYD, LUC,NUT	5,98
J	Coastal wetland burial	60	−	Land	Nearshore	CUC	5
K	Burial in tidal flats and deltas	50	?	Land	Nearshore	CC, HYD,LUC	5,99

'Nearshore' is equivalent to 'estuaries and coastal vegetated ecosystems,' while 'margins' correspond to 'continental shelves'. The continental 'shelf mask' that we are using covers 28 million km² and unambiguously excludes estuaries and anything upstream[99]. Figure 1 codes are letters with process representation plotted in Fig. 1. Signs for flux with perturbation indicate whether anthropogenic activities have increased (+) or decreased (−) the POC fluxes (? denotes direction of change unknown). Source of anthropogenic perturbations: CC, climate and CO_2 increase; LUC, Land-use change; NUT, enhanced nutrients to aquatic systems; HYD, water management; CUC, coastal use change (for example, reduction in coastal vegetated areas).

late twentieth- and twenty-first-century increases in land-use changes in South America, Africa and Southeast Asia have made these tropical areas the main loci of soil erosion, with rates predicted to substantially increase in the near future[12]. Human-induced, extreme precipitation/flooding events are also predicted to increase in many regions across the world (for example, ref. 21), affecting erosion rates and the fate of mud–OC[12].

Fate of mud–OC along the global inland water network

Humans clearly affect the mobilization, processing and storage of mud–OC in the transit from soils to the ocean, especially via the residence time of mud in different parts of the system[3,22–24]. Dam proliferation in North America, Europe/Eurasia and Asia since the 1950s is generally believed to be starving the coast of sediment (Supplementary Fig. 1). In contrast, sediment transport in 39% of rivers in South America, Africa and Oceania has increased since the 1980s due to land-use changes, especially deforestation[25]. Current estimates indicate a 49% global reduction in fluvial sediment reaching the oceans, despite a >200% increase in upstream fluvial sediment loads, between 1950 and 2010[11,25]. Dams can trap mud–OC (60 TgC yr⁻¹, range 20–70 TgC yr⁻¹; Figs. 1 and 2c, and Table 1)[26], the magnitude of which depends upon specific environmental and hydrological conditions (for example, refs. 26,27). For instance, dams strongly stimulate phytoplanktonic production within the global inland water network, but also the mineralization of both fresh OM and terrestrial-derived material; thus these systems exhibit a highly variable, net heterotrophic status at the global scale[27]. Dam construction up to 1970 eliminated 8% of the total riverine OC flux through burial and mineralization, and this removal rate is expected to have more than doubled (to 19% in 2030) with dams either completed or planned after 1970[27]. Furthermore, the interruption of sediment flux by dams increases net downstream erosion (Fig. 2c), which can partially offset mud–OC trapping until the river profile re-equilibrates (for example, ref. 28). Lakes without dams are also important hotspots of mud–OC burial (90 TgC yr⁻¹, range 40–180 TgC yr⁻¹; Fig. 1 and Table 1), although substantially less efficient on an areal basis than reservoirs with higher sedimentation rates and better conditions for OC preservation (for example, anoxia; Box 2)[26]. Moreover, several regional studies suggest a substantial increase in lake mud–OC burial since pre-industrial times[5]. Northern Hemisphere lakes have increased OC burial by about 50% over the past century (Fig. 2c), possibly due to the combined effects of climate change and enhanced terrestrial productivity[29]. Present-day OC accumulation rates in European lakes are double those of the Holocene, mostly attributed to land-use change[30].

River floodplains are key areas of storage, processing and release of mud–OC, affecting OC:SSA values and OC reactivity. As with reservoirs, they lead to mixtures of new and 'aged' materials[3,4]. In contrast to lakes and reservoirs for which global assessments of long-term burial are available (for example, ref. 26), the amount of mud–OC sequestered in floodplain systems is highly uncertain but possibly of similar magnitude (190 TgC yr⁻¹, range 60–320 TgC yr⁻¹)[5,31] as in lentic bodies (150 TgC yr⁻¹, range 60–250 TgC yr⁻¹; Fig. 1 and Table 1). Natural floodplains store and release mud via overbank sedimentation and river channel migration/river bank erosion, respectively, as well as other climate-driven fluctuations in the hydrological cycle (for example, La Niña and El Niño). Levee construction interrupts this process, often by reducing connectivity between rivers and their floodplains (for example, ref. 32). Increased erosion from human activities may reduce mud residence times in the land–ocean transition (Fig. 2b), but the creation and isolation of floodplains has the opposite effect[33]. The net effects of human activities on the floodplain mud–OC cycle remain largely unknown at the global scale (see ref. 5). While the composition of mud minerals varies relatively little during the long transit from source to sink, as evidenced by similar oceanic and adjacent terrestrial clay mineral suites[34], the composition of mud–OC is more variable[35,36]. Much mud–OC is decomposed in floodplains in its transit[23,37]. Along the entire source-to-sink transition, but particularly in the floodplain, petrogenic OM is partially replaced by OC from land plants and river/lake phytoplankton (for example, refs. 23,27). The addition of fresh OM may prime the degradation and replacement observed in floodplains[38].

Changes in fluvial morphology affect the fate of mud–OC by altering water dynamics, residence time, redox conditions, turbidity, particle size/density and mineral/OC sources[39]. Agricultural expansion in river networks in China (1960s–1980s) enhanced erosion and resulted in the loss of high-order rivers to sediment infilling[40]. During later urbanization (1980s–2010s), when ca. 40% of some natural landscapes reached a status of 'urbanized' (for example, extensive dredging and reconstruction of high-order rivers), lower-order rivers experienced sediment infilling. The importance of changing floodplain topography on mud–OC cycling remains largely unexplored (for example, ref. 41). The creation of reclaimed agricultural land such as rice paddies (Supplementary Fig. 1) can enhance OC:SSA ratios several fold[42]. Greater predictability in the land-use-driven changes in river channel evolution and spatial–temporal dynamics of erosion and sedimentation across
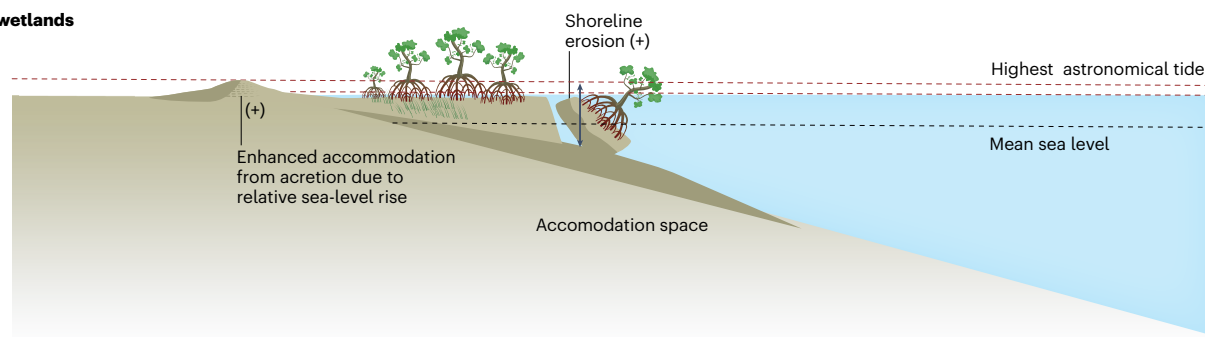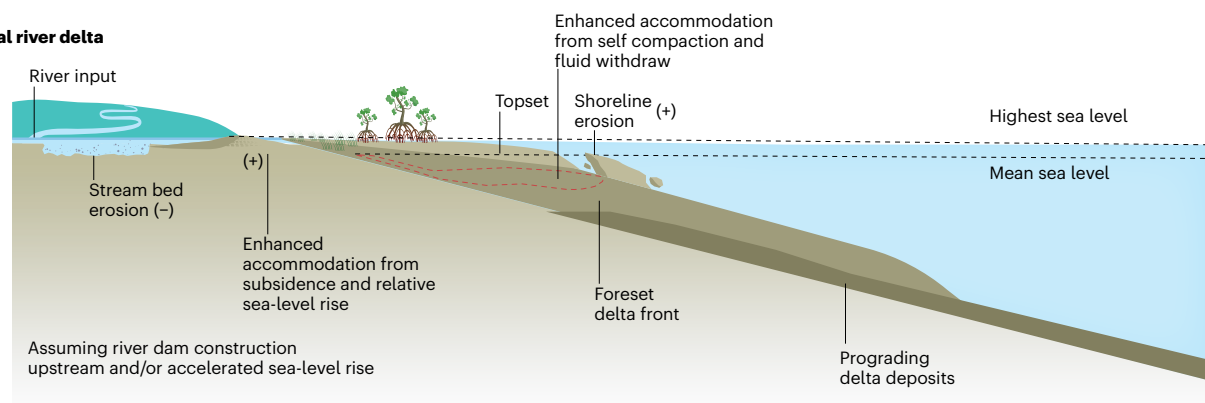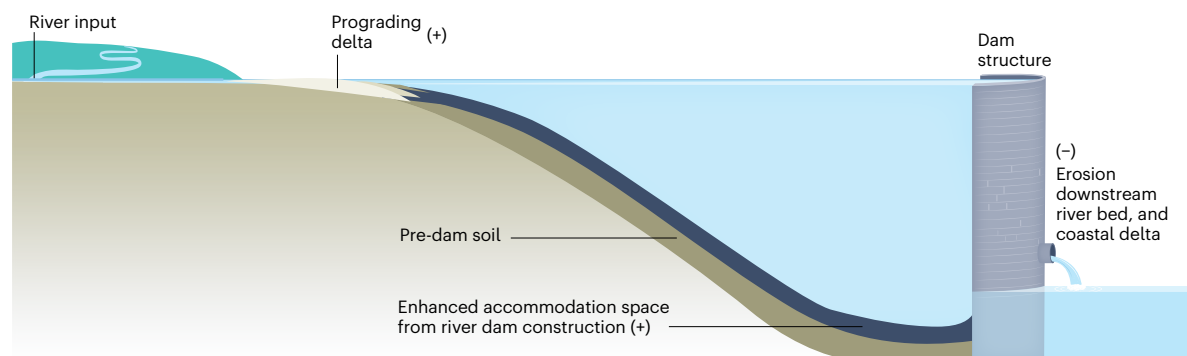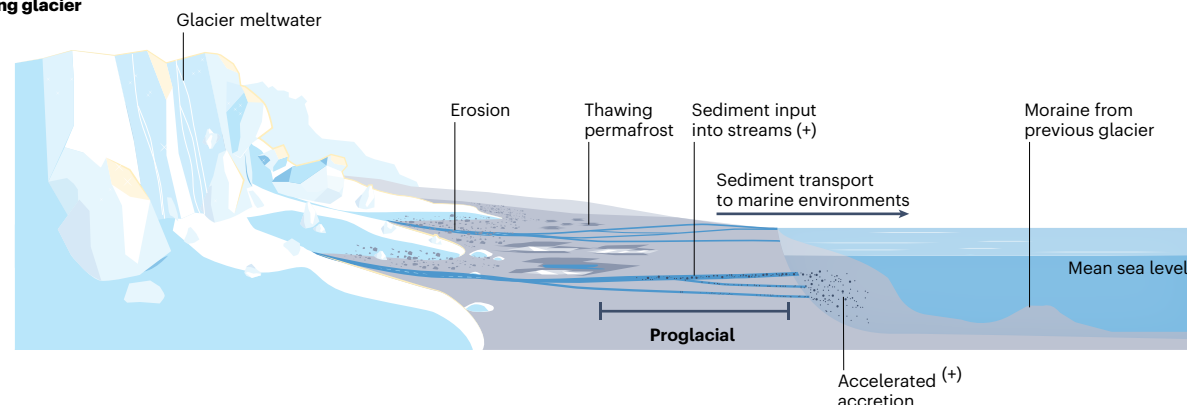
Fig. 2 | Examples of major perturbations of mud–OC pathways.
a,b, Accommodation space for vegetated coastal ecosystems (**a**) and deltas (**b**) is affected by the changing influence of sea level, sediment accumulation rate and vertical ground motion. **c,d**, Sediment transport pathways are being altered by anthropogenic alterations, such as dam construction (**c**), and climate warming and impacts to coastal environments (**d**). Plus and negative signals represents increments (+) or reductions (−) in mud–OC fluxes from/to accommodation space associated with different processes that have been altered during the Anthropocene.

BOX 2

Mud–OC reactivity in the Anthropocene

The reactivity of OC is highly variable and controlled by a plethora of different factors such as OM composition, electron acceptor availability, benthic microbial community composition, physical and physicochemical protection, temperature, microbial inhibition by specific chemicals, priming, and macrobenthic activity. Compiled OC reactivities (for example, apparent first-order OM degradation rate constant k, for OM of concentration G degrading according to a first-order rate law of the type $dG/dt=-kG$) correlate inversely with exposure to degradation time t across highly different environments (Fig. 3), despite inherent variability from a mixture of observations, lab and modelling data, as well as different approaches in calculating 'degradation time'. Depositional environments characterized by high, turbulent kinetic energy (enhanced lateral transport), phytodetrital aggregates or mesoscale fronts with enhanced downward transport (enhanced vertical transport) often reveal unusually high apparent benthic OM reactivity (for example, refs. 88,89). Interestingly, the one to two order of magnitude variances in OC reactivity (y axis, Fig. 3) at various places along the x axis look consistent across very different environments (for example, lake sediment versus wetland) at the century scale. However, human activity such as damming might shunt a certain-age mud from coastal environments that perform as oxidizers to riverine reservoirs of mud–OC. Thus, humans can upshift or downshift the regression line of OC reactivity for any given age of material. Changing the residence time of mud therefore puts 'a hold' on mud and mud–OC into a different reactivity environment for a new time period. That said, one could shift the apparent 'age' of OC by adding younger OC (for example, autotrophic OC) that would affect the apparent ages from which the plot is constructed. For example, ocean sediment rate constants appear lower than lake sediment ones for smaller than decadal timescales, perhaps due to greater depths of ocean sediments receiving less modern or lower fraction modern (Fm) OC; Fm is the ^{14}C abundance relative to 95% of the activity of NBS oxalic acid-I in 1950. However, it remains very difficult to predict how this would ultimately affect the $x–y$ regression in Fig. 3 as these effects will vary in intensity and will probably be environment-specific.

A notable example of how humans can rapidly alter the reactivity spectrum of OC across a source-to-sink gradient is the Arctic release of highly reactive, millennial-aged permafrost (for example, ref. 9). If we assume that a certain fraction of OC will persist (for example, will not be accessible on the defined timescale), then changes in transport timescales and environmentally driven changes in degradation rates will have little or no effect on its fate. As an example, enhanced downward transport of fresh planktonic OM can have multiple effects on the diagram. One might be via priming (for example, ref. 38), and thus accelerating decay of already-present OM. A second might be to induce bottom water anoxia and reduce the reactivity k of all of the sedimentary OM.

world's larger deltas (for example, those with areas >1,000 km² such as the Mississippi, Mekong and so on)[45], which are sinking several times faster than smaller deltas because they are downstream of more dams, contain higher fractions of compressible mud in areas large enough to induce isostatic subsidence[11] and are extensively modified by humans. In contrast, many (mostly smaller) coastal deltas have grown over recent decades, largely due to increases in fluvial-derived sediment linked to deforestation[46]. Century-long records show a doubling of sediment accumulation rates in most North American coastal depocentres apart from the Mississippi Delta region, facilitated by erosion downstream of dams[47] (Fig. 2c).

Coastal deltas and estuaries (Fig. 2a,b) are key depositional and processing environments of mud–OC along the source-to-sink transition, where unidirectional river flow interfaces with tidal and wave processes (for example, ref. 48). Despite complexity among coastal regions, sea-level rise and extensive coastal development have resulted in a net global decrease in mudflat area, primarily in temperate and low-latitude regions (Supplementary Fig. 1)[49]. Over two decades (1999–2019), an estimated 13,700 km² of tidal wetlands were lost globally, offset by gains of 9,700 km², for a global net loss of 4,000 km² (ref. 50). Coastal wetlands (Fig. 2a), which commonly host 'blue carbon' (for example, mangroves, tidal marshes and seagrasses; Supplementary Fig. 1), can have very high OC:SSA values (for example, up to 34 mgOC m⁻²)[51,52] and have some of the highest rates of short-term carbon sequestration and mud–OC burial (for example, ref. 53), with a global assessment reaching 60 TgC yr⁻¹ (range 40–80 TgC yr⁻¹; Fig. 1 and Table 1)[5].

In fast-warming pan-Arctic latitudes, permafrost thaw and thermo-erosional features in coastal regions have remobilized soils and changed source-to-sink movement of mud–OC (for example, refs. 54,55). While the range of grain size in permafrost can be quite variable, recent studies have shown that the majority of soil OC in permafrost across the Arctic is in the mud fraction[56,57]. Warming air and sea temperatures, sea-level rise and longer open-water seasons have enhanced pan-Arctic erosion and mobilization by 14 TgOC yr⁻¹ from permafrost soils to the aquatic continuum[54,58] (Figs. 1 and 2d, and Table 1). In turn, the mobilization of this old mud–OC and associated nutrients sustains a substantial fraction of Arctic primary production and supply of new fresh OM[59]. Much of the permafrost OC comprises silty mud–OC draining from nearshore erosion of retrogressive thaw slumps and bluffs/cliffs[60]. Mud–OC export from retrogressive thaw slumps, which typically extend farther inland than cliffs, may take decades to hundreds of years, compared with days to months from cliffs, before reaching the Arctic Ocean[54]. These differences in OC release result in a slower and steady conversion to CO_2 from retrogressive thaw slumps, compared with more rapid pulses of cliff-derived mud–OC release[54]. Pan-Arctic coastal systems also provide more targeted zones for examining the impact of ocean phytoplankton on the fate of permafrost-derived mud–OC in a warming climate. For example, mud–OC in deep waters of non-glaciated fjords of southeastern Alaska is largely undegraded with modern radiocarbon ages (biospheric sources), due to inputs of phytoplankton[61]. In contrast, nearby glaciated fjords are starved of phytoplankton and bury substantial amounts of petrogenic OC and terrigenous biospheric OC (Fig. 2d). Similar to cliff and retrogressive thaw slump systems, Arctic deltas represent an important land–sea interface, where thawed, millennial-aged, permafrost-derived mud–OC is processed. For example, permafrost-derived mud–OC in the Colville River delta, Alaska, originates from bank erosion in upstream tributaries in the basin[55] (Fig. 2d). How glacial retreat in the Arctic affects mud–OC burial will largely depend on regional differences in sedimentation rates, the relative inputs of older terrestrial sources (for example, petrogenic, permafrost) versus younger marine (macro- and microalgal), differential binding of these OC sources to minerals and the response of the microbial community to these changing pools.
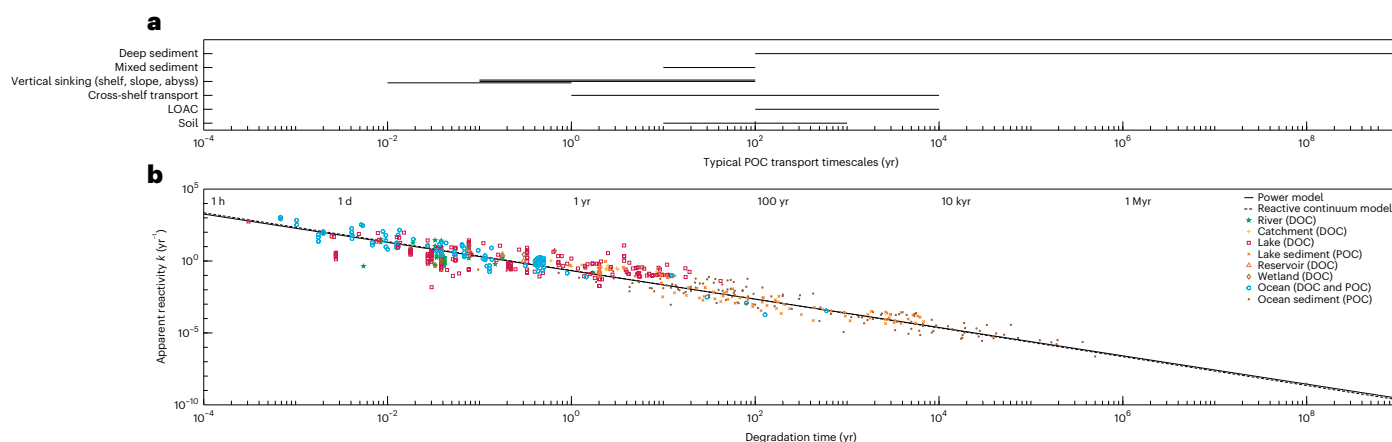
watersheds[43] will provide consistent frameworks to assess changes in mud–OC[44].

Production, transfer and storage of mud–OC at the coast

In addition to impacts on terrestrial sediment and mud–OC fluxes, damming has contributed to coastal erosion (Fig. 2) in many of the

Fig. 3 | Gradients of mud–OC reactivity. a, Typical mud–OC transport timescales for the transit through different environments as derived from radiocarbon measurements (for example, soil[102], land–ocean aquatic continuum (LOAC)[103–105] and shelf[106,107]) calculated based on vertical sinking rates (shelf, slope and abyss) and burial rates (marine mixed sediment, marine deep sediment). Vertical sinking zones listed on the y axis are as follows: shelf (0–200 m), slope (200–3,000 m) and abyss (>3,000 m). **b**, Distribution of apparent OM reactivity as derived from observations, model fitting and/or laboratory experiments for POC and dissolved OC (DOC) across different environments over degradation time (for example, river, catchment, lake, reservoir, wetland[108]) and ocean (sediment traps[109], sediment[109,110]). The first-order degradation rate constant, k, predicted for the respective exposure times by the reactive continuum model model ($k = 0.125\,(0.56\ \text{years} + \text{exposure time})^{-1}$) and the power model ($k = 0.21 \times$ exposure time$^{(-0.985)}$) are indicated by the dashed and solid line, respectively. We use 'degradation time' rather than 'time' as time could in theory pass without degradation proceeding (for example, permafrost or redox fluctuations or temporary mineral protection).

Accommodation space in nearshore coastal ecosystems

Accommodation space is space available for vertical mineral and organic material accumulation in nearshore ecosystems (for example, coastal wetlands, deltas, estuaries, inner shelves). It is largely controlled by relationships between sea level, sediment accumulation rate and vertical ground motion (for example, isostatic adjustment, tectonics, subsidence/sediment compaction and fluid withdrawal; for example, ref. 62; Figs. 1 and 2a,b). However, dramatic anthropogenic alterations in the delivery of fluvial sediments to the coast[11] and structures from human development[63] also change available accommodation space, which affects potential storage and turnover of mud–OC (Fig. 2a,b).

Modelling and empirical data suggest that accommodation space is a key variable determining coastal wetland habitat (Fig. 2a) expansion during sea-level rise over the past few millennia[64]. Recent models show that, over the past ca. 4,200 years, tidal marshes in regions with more rapidly declining relative sea-level rise (for example, Europe and North America) had greater OC concentration than in regions with slower declining relative sea-level rise (for example, Africa, Australia, China and South America)[65]. In the case of the Northern Hemisphere, where relative sea-level rise has been decelerating, vertical and lateral accommodation space was created over time[66], due to greater inundation frequency that allowed for higher mud–OC accumulation[64]. Controls on accommodation space are further complicated in large deltaic regions experiencing anthropogenic disturbances (Figs. 1 and 2b). For example, these regions experience high rates of erosion and subsidence, largely due to upstream damming and deltaic activities such as fossil fuel and groundwater extraction, respectively (for example, ref. 67). The synergistic effects of damming and subsidence increase relative sea-level rise in these deltaic regions, and further complicate modelling efforts of changing lateral and vertical accommodation space and associated mud–OC storage[68]. Damming also enhances accommodation space for storage of mud–OC in reservoirs (Figs. 1 and 2c).

Accommodation space in the Arctic coastal zone is also changing, as many glaciers (Figs. 1 and 2d, and Table 1), especially tidewater glaciers, experience rapid retreat[69]. This retreat poses new questions of how plant colonization will impact the erosion and development of soils, and hence mud–OC, in newly exposed proglacial deposits (sometimes termed paraglacial)[70]. For example, the development of coastal landforms (deltas, cliffs, tidal flats, beaches) in proglacial deposits over the past 100 years in Svalbard, Norway[71], provides new accommodation space for producing and processing mud–OC in the Arctic (Fig. 2d), and over relatively short periods of time (10^{-1} to 10^2 years). Tidal glacier retreat creates proglacial landforms that potentially increase accommodation space, which can then increase residence time (in part, stabilized by shrubification) and microbial processing of mud–OC in source-to-sink transport. Newly exposed glacial sediment can show rapid increase in OC:SSA ratios[72]. To date, much of what is known about primary succession of plants in these temperate-to-Arctic environments is from dated chronosequences from post-glacial retreat following the Little Ice Age[73].

Production, transfer and storage of offshore mud–OC

Muddy ocean deposits dominate longer-term processing and storage of mud–OC[22]. Organic loadings per unit of mud, as indicated by OC:SSA ratios, vary among depositional sites within an ocean margin region, depending on local ratios of supply versus degradation rates of mud–OC[3,74]. The burial or oxidation fate of enormous quantities of terrigenous OC depends on local oceanographic conditions. For example, the 1,600-km-long inner shelf mud belt, which moves from the mouth of the Amazon River to the Orinoco Delta, efficiently oxidizes terrigenous mud–OC, as energetic transport lowers OC:SSA ratios several fold via frequent resuspension and re-oxidation of the seabed[75]. In contrast, the offshore Ganges–Brahmaputra and Congo River outflows exhibit seaward escape of sediment via turbidity currents in submarine canyons and efficient terrigenous mud–OC burial on the adjacent deep-sea fan[23]. One of the more dramatic examples of human impacts on the distribution of mud–OC is the state change from actively accreting to eroding expansive shelf mud blankets. For example, humans and climatic variations interacted to control Holocene mud flux from mid-latitude Chinese loess hills to the adjacent ocean margin[76]. Recently, the underwater delta off the Yangtze has been rapidly eroding in response to river damming that captures sediment upstream[77], and that will surely impact biogeochemical processes and elemental fluxes for the East China Sea. Future planned dams in the

Amazon basin will probably dampen the extensive offshore mobile mud belts and mud–OC oxidation[78].

Along the ocean margins, the human impacts on mud–OC burial driven by changes in terrigenous OC deliveries are confounded by anthropogenic perturbations to ocean phytoplanktonic productivity. These include the effects of a changing physical climate and changes in nutrient inputs from atmospheric and riverine sources. Although it has long been advocated that human activities have stimulated ocean productivity and OC burial in the shallow portions of the ocean (for example, ref. 79), only recently have these impacts been quantified using physically resolved ocean biogeochemistry models[80]. Results suggest that over the Anthropocene, net coastal ocean productivity increased by 14% as a result of nutrient inputs, and was higher in hot-spot regions such as the East China Sea, southern North Sea, Louisiana shelf and shelves of the Bay of Bengal[80]. These results confirm reported widespread increases in biological productivity and eutrophication in coastal regions over the past century[81], probably inducing greater export, deposition and burial of mud–OC. With low confidence, the effects of a changing physical climate in the coastal ocean appear limited so far. The confounding effects of changing terrestrial and marine carbon cycles driven by multiple human factors (land-use change, climate, atmospheric CO_2, nutrient supply) make quantitative assessment of net changes in OC storage in muddy ocean sediments challenging[5]. Elevated OC:SSA ratios are evident in smaller eutrophied areas such as Long Island Sound[74], but not in larger, more exposed environments such as the East China Sea or Mississippi Delta[82]. This contrast suggests human impacts on OC decay may be more important than those on OC supply.

Mud–OC reactivity across a changing source-to-sink gradient

First-order degradation rate constants (k for a first-order rate law of the type $dG/dt = -kG$, with k denoting the first-order rate constant, G the OM concentration of natural OM and t is time) vary by many orders of magnitude, with a strong inverse relationship (over 12 orders of magnitude of time) in which OM is exposed to oxidizing or remineralizing conditions[83,84] (Fig. 3). This global observation broadly supports the widely accepted 'aged OC is refractory relative to recently produced OC' paradigm. It does not directly provide a mechanistic explanation of the long-term persistence of OC in the environment, although it can be summarized via integrative parameters such as energies of activation[85]. Superimposed on this broad trend is one to three orders of magnitude variation in reactivity at any given time of exposure. This variation is probably owing in part to varying definitions of time and reactivity arising from different data sources or models. It is also certainly subject to a plethora of different factors such as OM composition, electron acceptor availability, benthic microbial community composition, physical and physicochemical protection, temperature, microbial inhibition by specific chemicals, priming, and macrobenthic activity (for example, ref. 86 and references therein). Nevertheless, apparent reactivity provides an averaging dynamic parameter, accounting for interactions of compositional and environmental effects (Box 2). Interactions between mud and mud–OC seem to be particularly important on degradation timescales longer than 10^0–10^1 years (ref. 87) that are particularly important to carbon sequestration[85].

Accelerated human activity in the Anthropocene acts on these reactivity controls. Climate shifts can thaw permafrost mud–OC and enhance microbial decay, or stratify water columns that can deplete bottom waters of oxygen and slow microbial attack under quiescent or resuspension conditions (for example, ref. 88). Shunting mud into zones subject to fresh OM inputs—such as eutrophic coastal waters, dammed reservoirs or floodplains—can enhance reactivity of aged mud–OC via priming[38]. Such upshifts and downshifts of reactivity have potentially large impacts on mud–OC reactivity, coupled to changing mud residence times among different depocentres.

Concluding remarks

Most mud–OC formed over timescales longer than those of the Anthropocene, during which human activities are destabilizing this pool. These recent changes have created a non-steady-state situation that contrasts substantially with the mid-Holocene epoch, when climate conditions (and erosion processes) were more stable[8,89]. Furthermore, human impacts have led to the 'release' of old mud–OC, via destabilization and erosion of the landscape, into the modern carbon cycle[4,90]. While much has been discussed about the thaw and release of millennial-aged OC in high latitudes and its consequences for climate, only recently have we begun to consider the impact of climate change on the stability of mud–OC in tropical settings. Furthermore, anthropogenic activities also mobilize and destabilize petrogenic mud–OC in catchments with steep terrains and OM-rich metasedimentary rocks[91].

Mud holds most sequestered OC and exerts an important control on both OC transport and reactivity. The spatiotemporal history of mud in source-to-sink systems controls their respective net carbon budget over a wide range of timescales. On geologic timescales, the balance between the oxidation of petrogenic mud–OC and the formation/stabilization of biospheric mud–OC can tip source-to-sink systems from net carbon sinks (for example, the Ganges–Brahmaputra[67]) to net carbon sources (for example, Taiwan[91]). Over much shorter, human timescales, the Great Acceleration[9] has caused substantial shifts in the environments of the mud medium, leading to rapid changes in its mud–OC content and composition. While grain-size normalization illuminates mud–OC changes in any grain-size matrix, future research might emphasize areas where large muddy OC fluxes are especially affected by humans—for example, muddy parts of floodplains (Fig. 1). Determination of changes in mud–OC content, source and composition relative to the conservative medium—rather than simple relocation of mud (for example, ref. 92)—will allow better accounting for dynamic carbon reservoirs such as blue carbon, with implications for our ability to predict the global short-term evolution of OC reservoirs and attendant trends in atmospheric CO_2 levels. New analytical methods geared towards obtaining fine-scale characterizations of the interactions between mud and mud–OC (for example, MAOC, ramped pyrolysis oxidation, Fe–OC, split flow thin cell technique) as well as data aggregation tools are leading to global scale quantification of these disturbances to previous values. Finally, we summarize that anthropogenic activities have increased net fluxes and/or burial of mud–OC from mountain glaciers, land erosion, dam and lake reservoirs, river export, permafrost thaw, ice-sheet erosion and coastal margins, with uncertain net changes for tidal flats and floodplains, and probably net decreases in coastal wetlands (Table 1). Whether these impacts predict future trends deserves mechanistic and budgetary study. Whether the anthropogenic mobilization of mud–OC results in more or less sequestration of OC is not known with the current data, as it is dependent on timescales that involve complex transient effects.

References

1. Deevey, E. S. In defense of mud. *Bull. Ecol. Soc. Am.* **51**, 5–8 (1970).

2. Malakoff, D. Mud. *Science* **369**, 894–895 (2020).

3. Blair, N. E. & Aller, R. C. The fate of terrestrial organic carbon in the marine environment. *Annu. Rev. Mar. Sci.* **4**, 401–423 (2012).

4. Eglinton, T. I. et al. Climate control on terrestrial biospheric carbon turnover. *Proc. Natl Acad. Sci. USA* **118**, e2011585118 (2021).

5. Regnier, P., Resplandy, L., Najjar, R. G. & Ciais, P. The land-to-ocean loops of the global carbon cycle. *Nature* **603**, 401–410 (2022).

6. Falkowski, P. G., Fenchel, T. & Delong, E. F. The microbial engines that drive Earth's biogeochemical cycles. *Science* **320**, 1034–1039 (2008).

7. Blatt, H. *Sedimentary Petrology* (1982).

8. Jenny, J.-P. et al. Human and climate global-scale imprint on sediment transfer during the Holocene. *Proc. Natl Acad. Sci. USA* **116**, 22972–22976 (2019).

9. Zhang, T. et al. Warming-driven erosion and sediment transport in cold regions. *Nat. Rev. Earth Environ.* **3**, 832–851 (2022).

10. Rosentreter, J. A. et al. Coastal vegetation and estuaries are collectively a greenhouse gas sink. *Nat. Clim. Change* **13**, 579–587 (2023).

11. Syvitski, J. et al. Earth's sediment cycle during the Anthropocene. *Nat. Rev. Earth Environ.* **3**, 179–196 (2022).

12. Borrelli, P. et al. An assessment of the global impact of 21st century land use change on soil erosion. *Nat. Commun.* **8**, 2013 (2017).

13. Ellis, E. C. et al. Used planet: a global history. *Proc. Natl Acad. Sci. USA* **110**, 7978–7985 (2013).

14. Klein Goldewijk, K., Beusen, A., Doelman, J. & Stehfest, E. Anthropogenic land use estimates for the Holocene–HYDE 3.2. *Earth Syst. Sci. Data* **9**, 927–953 (2017).

15. Kemp, D. B., Sadler, P. M. & Vanacker, V. The human impact on North American erosion, sediment transfer, and storage in a geologic context. *Nat. Commun.* **11**, 6012 (2020).

16. Zhang, F. et al. Human impacts overwhelmed hydroclimate control of soil erosion in china 5,000 years ago. *Geophys. Res. Lett.* **49**, e2021GL096983 (2022).

17. Winkler, K., Fuchs, R., Rounsevell, M. & Herold, M. Global land use changes are four times greater than previously estimated. *Nat. Commun.* **12**, 2501 (2021).

18. Panagos, P. et al. Projections of soil loss by water erosion in Europe by 2050. *Environ. Sci. Policy* **124**, 380–392 (2021).

19. Li, G. et al. Dam-triggered organic carbon sequestration makes the Changjiang (Yangtze) River basin (China) a significant carbon sink. *J. Geophys. Res. Biogeosci.* **120**, 39–53 (2015).

20. Zhang, H. et al. Global changes alter the amount and composition of land carbon deliveries to European rivers and seas. *Commun. Earth Environ.* **3**, 245 (2022).

21. IPCC *Climate Change 2022: Impacts, Adaptation and Vulnerability* (eds Pörtner, H.-O. et al.) (Cambridge Univ. Press, 2022).

22. Bianchi, T. S. et al. Centers of organic carbon burial and oxidation at the land–ocean interface. *Org. Geochem.* **115**, 138–155 (2018).

23. Galy, V. et al. Efficient organic carbon burial in the Bengal fan sustained by the Himalayan erosional system. *Nature* **450**, 407–410 (2007).

24. Kuehl, S. A. et al. Asia's mega rivers: common source, diverse fates. *Eos* 10.1029/2020EO143936 (2020).

25. Dethier, E. N., Renshaw, C. E. & Magilligan, F. J. Rapid changes to global river suspended sediment flux by humans. *Science* **376**, 1447–1452 (2022).

26. Mendonca, R. et al. Hydroelectric carbon sequestration. *Nat. Geosci.* **5**, 838–840 (2012).

27. Maavara, T., Lauerwald, R., Regnier, P. & Van Cappellen, P. Global perturbation of organic carbon cycling by river damming. *Nat. Commun.* **8**, 15347 (2017).

28. Charoenlerkthawin, W. et al. Effects of dam construction in the Wang River on sediment regimes in the Chao Phraya River basin. *Water* **13**, 2146 (2021).

29. Heathcote, A. J., Anderson, N. J., Prairie, Y. T., Engstrom, D. R. & Del Giorgio, P. A. Large increases in carbon burial in northern lakes during the Anthropocene. *Nat. Commun.* **6**, 10016 (2015).

30. Kastowski, M., Hinderer, M. & Vecsei, A. Long-term carbon burial in European lakes: analysis and estimate. *Glob. Biogeochem. Cycles* https://doi.org/10.1029/2010GB003874 (2011).

31. Hoffmann, T. O. in *Treatise on Geomorphology* 2nd edn (ed. Shroder, J. F.) 458–477 (Academic Press, 2022).

32. Grill, G. et al. Mapping the world's free-flowing rivers. *Nature* **569**, 215–221 (2019).

33. Lewin, J. & Ashworth, P. J. The negative relief of large river floodplains. *Earth-Sci. Rev.* **129**, 1–23 (2014).

34. Blattmann, T. M. Mineralogical control on the fate of continentally derived organic matter in the ocean. *Science* **366**, 742–745 (2019).

35. Repasch, M. et al. Fluvial organic carbon cycling regulated by sediment transit time and mineral protection. *Nat. Geosci.* **14**, 842–848 (2021).

36. Repasch, M. et al. River organic carbon fluxes modulated by hydrodynamic sorting of particulate organic matter. *Geophys. Res. Lett.* **49**, e2021GL096343 (2022).

37. Scheingross, J. S. et al. The fate of fluvially-deposited organic carbon during transient floodplain storage. *Earth Planet. Sci. Lett.* **561**, 116822 (2021).

38. Bianchi, T. S. The role of terrestrially derived organic carbon in the coastal ocean: a changing paradigm and the priming effect. *Proc. Natl Acad. Sci. USA* **108**, 19473–19481 (2011).

39. Grant, K. E., Galy, V. V., Haghipour, N., Eglinton, T. I. & Derry, L. A. Persistence of old soil carbon under changing climate: the role of mineral–organic matter interactions. *Chem. Geol.* **587**, 120629 (2022).

40. Wu, L. et al. Impacts of land use change on river systems for a river network plain. *Water* **10**, 609 (2018).

41. Aufdenkampe, A. K. et al. Riverine coupling of biogeochemical cycles between land, oceans, and atmosphere. *Front. Ecol. Environ.* **9**, 53–60 (2011).

42. Wissing, L. et al. Organic carbon accumulation on soil mineral surfaces in paddy soils derived from tidal wetlands. *Geoderma* **228**, 90–103 (2014).

43. Julian, J. P., Wilgruber, N. A., de Beurs, K. M., Mayer, P. M. & Jawarneh, R. N. Long-term impacts of land cover changes on stream channel loss. *Sci. Total Environ.* **537**, 399–410 (2015).

44. Golombek, N. Y. et al. Fluvial organic carbon composition regulated by seasonal variability in lowland river migration and water discharge. *Geophys. Res. Lett.* **48**, e2021GL093416 (2021).

45. Tessler, Z. D., Vörösmarty, C. J., Grossberg, M., Gladkova, I. & Aizenman, H. A global empirical typology of anthropogenic drivers of environmental change in deltas. *Sustain. Sci.* **11**, 525–537 (2016).

46. Nienhuis, J. H. et al. Global-scale human impact on delta morphology has led to net land area gain. *Nature* **577**, 514–518 (2020).

47. Rodriguez, A., McKee, B., Miller, C., Bost, M. & Atencio, A. Coastal sedimentation across North America doubled in the 20th century despite river dams. *Nat. Commun.* **11**, 3249 (2020).

48. van de Lageweg, W. I., Braat, L., Parsons, D. R. & Kleinhans, M. G. Controls on mud distribution and architecture along the fluvial-to-marine transition. *Geology* **46**, 971–974 (2018).

49. Murray, N. J. et al. The global distribution and trajectory of tidal flats. *Nature* **565**, 222–225 (2019).

50. Murray, N. J. et al. High-resolution mapping of losses and gains of Earth's tidal wetlands. *Science* **376**, 744–749 (2022).

51. Pinsonneault, A. J. et al. Dissolved organic carbon sorption dynamics in tidal marsh soils. *Limnol. Oceanogr.* **66**, 214–225 (2021).

52. Ilgen, A. G. et al. Shales at all scales: exploring coupled processes in mudrocks. *Earth-Sci. Rev.* **166**, 132–152 (2017).

53. Macreadie, P. I. et al. The future of blue carbon science. *Nat. Commun.* **10**, 3998 (2019).

54. Tanski, G. et al. Permafrost carbon and CO_2 pathways differ at contrasting coastal erosion sites in the Canadian Arctic. *Front. Earth Sci.* https://doi.org/10.3389/feart.2021.630493 (2021).

55. Zhang, X. et al. Recent warming fuels increased organic carbon export from Arctic permafrost. *AGU Adv.* **2**, e2021AV000396 (2021).

56. Schirrmeister, L. The genesis of Yedoma Ice Complex permafrost – grain-size endmember modeling analysis from Siberia and Alaska. *EG Quat. Sci. J.* **69**, 33–53 (2020).

57. Palmtag, J. & Kuhry, P. Grain size controls on cryoturbation and soil organic carbon density in permafrost-affected soils. *Permafr. Periglac. Process.* **29**, 112–120 (2018).

58. Vonk, J. E. Activation of old carbon by erosion of coastal and subsea permafrost in Arctic Siberia. *Nature* **489**, 137–140 (2012).

59. Terhaar, J., Lauerwald, R., Regnier, P., Gruber, N. & Bopp, L. Around one third of current Arctic Ocean primary production sustained by rivers and coastal erosion. *Nat. Commun.* **12**, 169 (2021).

60. Cunliffe, A. M. Rapid retreat of permafrost coastline observed with aerial drone photogrammetry. *Cryosphere* **13**, 1513–1528 (2019).

61. Cui, X., Bianchi, T. S., Jaeger, J. M. & Smith, R. W. Biospheric and petrogenic organic carbon flux along southeast Alaska. *Earth Planet. Sci. Lett.* **452**, 238–246 (2016).

62. Jervey, M. T. in *Sea-Level Changes: An Integrated Approach* (eds Wilgus, C. K. et al.) (SEPM Society for Sedimentary Geology, 1988).

63. Enwright, N. M., Griffith, K. T. & Osland, M. J. Barriers to and opportunities for landward migration of coastal wetlands with sea-level rise. *Front. Ecol. Environ.* **14**, 307–316 (2016).

64. Rogers, K. et al. Wetland carbon storage controlled by millennial-scale variation in relative sea-level rise. *Nature* **567**, 91–95 (2019).

65. Ouyang, X. & Lee, S. Updated estimates of carbon accumulation rates in coastal marsh sediments. *Biogeosciences* **11**, 5057–5071 (2014).

66. Schuerch, M. et al. Future response of global coastal wetlands to sea-level rise. *Nature* **561**, 231–234 (2018).

67. Brown, S. & Nicholls, R. J. Subsidence and human influences in mega deltas: the case of the Ganges–Brahmaputra–Meghna. *Sci. Total Environ.* **527**, 362–374 (2015).

68. Meselhe, E., White, E., Wang, Y. & Reed, D. Uncertainty analysis for landscape models used for coastal planning. *Estuar. Coast. Shelf Sci.* **256**, 107371 (2021).

69. Roe, G. H., Baker, M. B. & Herla, F. Centennial glacier retreat as categorical evidence of regional climate change. *Nat. Geosci.* **10**, 95–99 (2017).

70. Losapio, G. et al. The consequences of glacier retreat are uneven between plant species. *Front. Ecol. Evol.* **8**, 616562 (2021).

71. Strzelecki, M. C. et al. New fjords, new coasts, new landscapes: the geomorphology of paraglacial coasts formed after recent glacier retreat in Brepollen (Hornsund, southern Svalbard). *Earth Surf. Process. Landf.* **45**, 1325–1334 (2020).

72. Dümig, A., Häusler, W., Steffens, M. & Kögel-Knabner, I. Clay fractions from a soil chronosequence after glacier retreat reveal the initial evolution of organo–mineral associations. *Geochim. Cosmochim. Acta* **85**, 1–18 (2012).

73. Cauvy-Fraunié, S. & Dangles, O. A global synthesis of biodiversity responses to glacier retreat. *Nat. Ecol. Evol.* **3**, 1675–1685 (2019).

74. Mayer, L. M. Surface area control of organic carbon accumulation in continental shelf sediments. *Geochim. Cosmochim. Acta* **58**, 1271–1284 (1994).

75. Aller, R. C. & Blair, N. E. Carbon remineralization in the Amazon–Guianas tropical mobile mudbelt: a sedimentary incinerator. *Cont. Shelf Res.* **26**, 2241–2259 (2006).

76. Ai, L. et al. How did the climate and human activities modulate the sedimentary evolution of the Central Yellow Sea Mud, China. *J. Asian Earth Sci.* **235**, 105299 (2022).

77. Luo, X., Yang, S., Wang, R., Zhang, C. & Li, P. New evidence of Yangtze Delta recession after closing of the Three Gorges Dam. *Sci. Rep.* **7**, 41735 (2017).

78. Nittrouer, C. A. et al. Amazon sediment transport and accumulation along the continuum of mixed fluvial and marine processes. *Annu. Rev. Mar. Sci.* **13**, 501–536 (2021).

79. Mackenzie, F. T., Ver, L. M. & Lerman, A. Century-scale nitrogen and phosphorus controls of the carbon cycle. *Chem. Geol.* **190**, 13–32 (2002).

80. Lacroix, F., Ilyina, T., Mathis, M., Laruelle, G. G. & Regnier, P. Historical increases in land-derived nutrient inputs may alleviate effects of a changing physical climate on the oceanic carbon cycle. *Glob. Change Biol.* **27**, 5491–5513 (2021).

81. Fennel, K. & Testa, J. M. Biogeochemical controls on coastal hypoxia. *Annu. Rev. Mar. Sci.* **11**, 105–130 (2019).

82. Yao, P. et al. Remineralization of sedimentary organic carbon in mud deposits of the Changjiang Estuary and adjacent shelf: implications for carbon preservation and authigenic mineral formation. *Cont. Shelf Res.* **91**, 1–11 (2014).

83. Hilton, R. G., Galy, A., Hovius, N., Horng, M.-J. & Chen, H. Efficient transport of fossil organic carbon to the ocean by steep mountain rivers: an orogenic carbon sequestration mechanism. *Geology* **39**, 71–74 (2011).

84. Bouchez, J. et al. Source, transport and fluxes of Amazon River particulate organic carbon: insights from river sediment depth-profiles. *Geochim. Cosmochim. Acta* **133**, 280–298 (2014).

85. Keil, R. G. & Mayer, L. M. in *Treatise on Geochemistry* (eds Holland, H .D. and Turekian, K. K.) 337–359 (Elsevier, 2014).

86. Arndt, S. et al. Quantifying the degradation of organic matter in marine sediments: a review and synthesis. *Earth-Sci. Rev.* **123**, 53–86 (2013).

87. Hemingway, J. D. et al. Mineral protection regulates long-term global preservation of natural organic carbon. *Nature* **570**, 228–231 (2019).

88. Arnarson, T. S. & Keil, R. G. Changes in organic matter–mineral interactions for marine sediments with varying oxygen exposure times. *Geochim. Cosmochim. Acta* **71**, 3545–3556 (2007).

89. Bruni, E. T. et al. Sedimentary hydrodynamic processes under low-oxygen conditions: implications for past, present, and future oceans. *Front. Earth Sci.* **10**, 886395 (2022).

90. Petit, J.-R. et al. Climate and atmospheric history of the past 420,000 years from the Vostok ice core, Antarctica. *Nature* **399**, 429–436 (1999).

91. Hilton, R. G. & West, A. J. Mountains, erosion and the carbon cycle. *Nat. Rev. Earth Environ.* **1**, 284–299 (2020).

92. Hemingway, J. D. et al. Microbial oxidation of lithospheric organic carbon in rapidly eroding tropical mountain soils. *Science* **360**, 209–212 (2018).

93. Hood, E., Battin, T. J., Fellman, J., O'Neel, S. & Spencer, R. G. M. Storage and release of organic carbon from glaciers and ice sheets. *Nat. Geosci.* **8**, 91–96 (2015).

94. Tian, H. et al. Increased terrestrial carbon export and CO_2 evasion from global inland waters since the preindustrial era. *Glob. Biogeochem. Cycles* **37**, e2023GB007776 (2023).

95. Mendonça, R. et al. Organic carbon burial in global lakes and reservoirs. *Nat. Commun.* **8**, 1694 (2017).

96. Galy, V., Peucker-Ehrenbrink, B. & Eglinton, T. Global carbon export from the terrestrial biosphere controlled by erosion. *Nature* **521**, 204–207 (2015).

97. Wadham, J. L. et al. Ice sheets matter for the global carbon cycle. *Nat. Commun.* **10**, 3567 (2019).

98. Middelburg, J. J. *Marine Carbon Biogeochemistry: A Primer for Earth System Scientists* (Springer, 2019).

99. Bauer, J. E. et al. The changing carbon cycle of the coastal ocean. *Nature* **504**, 61–70 (2013).

100. LaRowe, D. E. et al. Organic carbon and microbial activity in marine sediments on a global scale throughout the Quaternary. *Geochim. Cosmochim. Acta* **286**, 227–247 (2020).

101. Bradley, J. A., Hülse, D., LaRowe, D. E. & Arndt, S. Transfer efficiency of organic carbon in marine sediments. *Nat. Commun.* **13**, 7297 (2022).

102. Faust, J. C. et al. Millennial scale persistence of organic carbon bound to iron in Arctic marine sediments. *Nat. Commun.* **12**, 275 (2021).

103. Suello, R. H. et al. Mangrove sediment organic carbon storage and sources in relation to forest age and position along a deltaic salinity gradient. *Biogeosciences* **19**, 1571–1585 (2022).

104. Gu, X. & Brantley, S. L. How particle size influences oxidation of ancient organic matter during weathering of black shale. *ACS Earth Space Chem.* **6**, 1443–1459 (2022).

105. Kennedy, M., Droser, M., Mayer, L. M., Pevear, D. & Mrofka, D. Late Precambrian oxygenation; inception of the clay mineral factory. *Science* **311**, 1446–1449 (2006).

106. Hage, S. et al. High rates of organic carbon burial in submarine deltas maintained on geological timescales. *Nat. Geosci.* **15**, 919–924 (2022).

107. Kleber, M. et al. Dynamic interactions at the mineral–organic matter interface. *Nat. Rev. Earth Environ.* **2**, 402–421 (2021).

108. Keiluweit, M., Gee, K., Denney, A. & Fendorf, S. Anoxic microsites in upland soils dominantly controlled by clay content. *Soil Biol. Biochem.* **118**, 42–50 (2018).

109. Curry, K. J. et al. Direct visualization of clay microfabric signatures driving organic matter preservation in fine-grained sediment. *Geochim. Cosmochim. Acta* **71**, 1709–1720 (2007).

110. Silburn, B. et al. Benthic pH gradients across a range of shelf sea sediment types linked to sediment characteristics and seasonal variability. *Biogeochemistry* **135**, 69–88 (2017).

111. Georgiou, K. et al. Global stocks and capacity of mineral-associated soil organic carbon. *Nat. Commun.* **13**, 3797 (2022).

112. Hedges, J. I. & Oades, J. M. Comparative organic geochemistries of soils and marine sediments. *Org. Geochem.* **27**, 319–361 (1997).

113. Potter, P. E., Maynard, J. B. & Depetris, P. J. *Mud and Mudstones: Introduction and Overview* (Springer, 2005).

114. Cai, C. et al. Occurrence of organic matter in argillaceous sediments and rocks and its geological significance: a review. *Chem. Geol.* **639**, 121737 (2023).

115. Bock, M. J. & Mayer, L. M. Mesodensity organo–clay associations in a near-shore sediment. *Mar. Geol.* **163**, 65–75 (2000).

116. Virto, I., Moni, C., Swanston, C. & Chenu, C. Turnover of intra-and extra-aggregate organic matter at the silt-size scale. *Geoderma* **156**, 1–10 (2010).

117. Blair, N. E., Leithold, E. L. & Aller, R. C. From bedrock to burial: the evolution of particulate organic carbon across coupled watershed–continental margin systems. *Mar. Chem.* **92**, 141–156 (2004).

Acknowledgements

Author contributions

T.S.B., L.M.M., J.H.F.A., S.A., V.G., D.B.K., S.A.K., N.J.M. and P.R. contributed to the conceptual development and writing of this paper. T.S.B., L.M.M and J.H.F.A. were key in leading the group through different stages of progress and revision. T.S.B., J.H.F.A., L.M.M., S.A., N.J.M. and P.R. contributed greatly to development and revisions of the table and figures.

Competing interests

The authors declare no competing interests.

Additional information

Supplementary information The online version contains supplementary material available at https://doi.org/10.1038/s41561-024-01405-5.

Correspondence and requests for materials should be addressed to Thomas S. Bianchi.

Peer review information *Nature Geoscience* thanks Marisa Repasch, Joel Scheingross and the other, anonymous, reviewer(s) for their contribution to the peer review of this work. Primary Handling Editor: Xujia Jiang, in collaboration with the *Nature Geoscience* team.

Reprints and permissions information is available at www.nature.com/reprints.